Four two-dimensional highly undulating silver(I)–hexamethylenetetramine co-ordination networks containing micropores

Shao-Liang Zheng, Ming-Liang Tong,* Hai-Liang Zhu and Xiao-Ming Chen*

School of Chemistry and Chemical Engineering, Zhongshan University, Guangzhou 510275, China. E-mail: cescxm@zsu.edu.cn; cestml@zsu.edu.cn

Received (in London, UK) 8th August 2001, Accepted 14th September 2001
First published as an Advance Article on the web 19th October 2001

Four interesting polymers, namely $[Ag_2(\mu_3\text{-hmt})_2(MeCN)](ClO_4)_2$ **1**, $[Ag(\mu_3\text{-hmt})(ma)]$ **2**, $[Ag(\mu_3\text{-hmt})(ba)]\cdot H_2O$ **3** and $[Ag(\mu_3\text{-hmt})(sal)]\cdot H_2O$ **4** (hmt = hexamethylenetetramine, ma = malonate, ba = benzoate and sal = salicylate) have been synthesised and structurally characterised by X-ray diffraction. In these complexes, the two-dimensional $[Ag(\mu_3\text{-hmt})]$ layers of hexagonal units are highly undulating and each pair of adjacent lateral ligands, MeCN or carboxylates, at the same side of the layers are slanted towards each other, resulting in intralayer micropores.

Introduction

The synthesis of co-ordination polymers with large channels or cavities has been rapidly expanding due to their intriguing structural diversity and potential applications as microporous solids for molecular adsorption, ion exchange, heterogeneous catalysis, and host–guest chemistry.[1] A number of infinite frameworks meet the requirements for such uses very well because the hosts employed are relatively rigid and contain large cavities and the van der Waals surfaces and electrostatic potential surfaces of the host and guest may be complementary.[2] Although a wide range of infinite one-, two- and three-dimensional microporous co-ordination frameworks have already been generated,[3,4] it is somewhat surprising that no two-dimensional microporous co-ordination frameworks based on corrugated sheets (Scheme 1) have been reported. Using a 'building block' methodology, combination of hexamethylenetetramine (hmt) as a potential tetradendate ligand and silver(I) has produced a wide variety of supramolecular architectures,[5–11] most of them made up of two-dimensional infinite wavy $[Ag(\mu_3\text{-hmt})]$ layers comprising hexagonal units in a boat-type conformation. It has been shown in our previous report[10] that with appropriate lateral ligands, such as nitro-substituted benzoate or linear dicarboxylates, the wavy $[Ag(\mu_3\text{-hmt})]$ layers of hexagonal units can be organised into three-dimensional molecular architectures through intercalation of the lateral aromatic ligands [Scheme 2(a, b)] or dicarboxylates as molecular pillars.[10] On the other hand, different types of interconnections between the hexagonal units in the two-dimensional $[Ag(\mu_3\text{-hmt})]$ layers may be expected to lead to different molecular architectures. So far, only one highly undulated two-dimensional $[Ag(\mu_3\text{-hmt})]$ layer with hexagonal units has been documented recently, namely that in $[Ag_2(\mu\text{-hmt})_2(CF_3SO_3)(H_2O)](CF_3SO_3)\cdot H_2O$.[6] Following on from our systematic investigation of Ag–hmt co-ordination networks, we now report here in four new co-ordination polymers, namely $[Ag_2(\mu_3\text{-hmt})_2(MeCN)](ClO_4)_2$ **1**, $[Ag(\mu_3\text{-hmt})(ma)]$ **2**, $[Ag(\mu_3\text{-hmt})(ba)]\cdot H_2O$ **3** and $[Ag(\mu_3\text{-hmt})(sal)]\cdot H_2O$ **4** (ma = malonate, ba = benzoate and sal = salicylate). In these complexes, the two-dimensional $[Ag(\mu_3\text{-hmt})]$ layers of hexagonal units in a boat-type conformation are highly undulating [Scheme 2(c, d)] and each pair of adjacent lateral ligands, MeCN or carboxylates, at the same side of the layers are slanted towards each other, resulting in new two-dimensional co-ordination frameworks comprising micropores, as illustrated in Scheme 1.

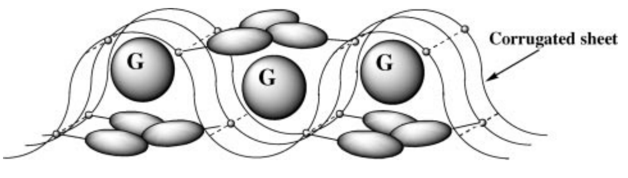

Scheme 1 Schematic representation of the topological motif of the two-dimensional microporous co-ordination layer based on a corrugated sheet.

Experimental

Materials

$AgClO_4$ was prepared by the reaction of Ag_2O and dilute $HClO_4$ solution, $Ag_2(ma)$, Ag(ba) and Ag(sal) were prepared

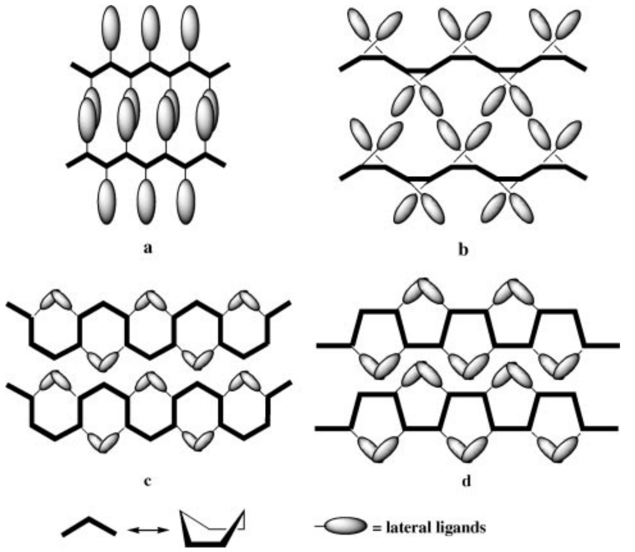

Scheme 2 Four interconnection modes of the hexagonal units in two-dimensional $[Ag(\mu_3\text{-hmt})]$ layers.

DOI: 10.1039/b107193a

Table 1 Crystal data and structure refinement for complexes **1**–**4**

Complex Formula	**1** $C_{14}H_{27}Ag_2Cl_2N_9O_8$	**2** $C_9H_{15}AgN_4O_4$	**3** $C_{13}H_{19}AgN_4O_3$	**4** $C_{13}H_{19}AgN_4O_4$
Fw	736.09	351.12	387.19	403.19
Crystal system	Orthorhombic	Orthorhombic	Orthorhombic	Orthorhombic
Space group	*Pbca* (no. 61)	*Pbca* (no. 61)	$Pca2_1$ (no. 29)	*Pbca* (no. 61)
a/Å	18.112(10)	11.488(3)	11.717(4)	11.620(6)
b/Å	10.860(5)	10.395(3)	11.741(6)	10.807(5)
c/Å	23.781(10)	19.527(7)	10.478(7)	23.145(12)
Volume/Å^3	4678(4)	2331.9(12)	1441.5(13)	2906(3)
Z	8	8	4	8
λ(Mo-Kα)/Å	0.71073	0.71073	0.71073	0.71073
T/K	293(2)	293(2)	293(2)	293(2)
ρ_{calc}/g cm^{-3}	2.090	2.000	1.784	1.843
μ(Mo-Kα)/mm^{-1}	1.965	1.743	1.414	1.412
No. of unique reflections	5486	2826	1908	2556
No. observed [$I \geqslant 2\sigma(I)$]	5103(0.0253)	2675(0.0577)	1745(0.0584)	2556(0.000)
Crystal size (mm)	0.44 × 0.38 × 0.34	0.42 × 0.36 × 0.24	0.42 × 0.32 × 0.18	0.42 × 0.36 × 0.28
R_1 [$I > 2\sigma(I)$]^a	0.0492	0.0527	0.0523	0.0566
wR_2 (all data)^a	0.1289	0.1540	0.1404	0.1362

[a] $R_1 = \Sigma \| F_o | - | F_c \| / \Sigma | F_o |$, $wR_2 = [\Sigma w(F_o^2 - F_c^2)^2 / \Sigma w(F_o^2)^2]^{1/2}$.

according to literature methods.[12] Other reagents and solvents employed were commercially available and used as received without further purification. The C, H, N microanalyses were carried out with a Perkin-Elmer 240 elemental analyser. The FT-IR spectra were recorded from KBr pellets in the range 4000–400 cm^{-1} on a Nicolet 5DX spectrometer. Thermogravimetric data were collected on a Perkin-Elmer TGS-2 analyser in flowing dinitrogen at a heating rate of 10 °C min^{-1}.

Syntheses

[Ag$_2$(μ$_3$-hmt)$_2$(MeCN)](ClO$_4$)$_2$ 1. An aqueous solution (5 cm^3) of hmt (0.14 g, 1.0 mmol) was added dropwise to a stirred MeCN–H$_2$O (2 : 1 *v*/*v*) solution (5 cm^3) of AgClO$_4$ (0.22 g, 1.0 mmol) 50 °C for 15 min. The mixture was dissolved by dropwise addition of aqueous NH$_3$ solution. The resulting pale yellow solution was allowed to stand in air at room temperature for two weeks, giving pale yellow crystals in good

Table 2 Selected bond lengths (Å) and angles (°) for complexes **1**–**4**^{a}

Complex **1**			
Ag(1)–N(6a)	2.347(5)	Ag(2)–N(8)	2.350(5)
Ag(1)–N(4b)	2.359(5)	Ag(2)–N(9)	2.360(7)
Ag(1)–N(5)	2.397(4)	Ag(2)–N(2)	2.380(5)
Ag(2)–N(3c)	2.349(5)		
N(6a)–Ag(1)–N(4b)	124.9(2)	N(3c)–Ag(2)–N(9)	96.3(3)
N(6a)–Ag(1)–N(5)	119.2(2)	N(8)–Ag(2)–N(9)	102.7(2)
N(4b)–Ag(1)–N(5)	114.3(2)	N(8)–Ag(2)–N(2)	110.6(2)
N(3c)–Ag(2)–N(2)	119.2(2)	N(9)–Ag(2)–N(2)	100.1(2)
N(3c)–Ag(2)–N(8)	122.0(2)		
Complex **2**			
Ag(1)–N(1)	2.345(4)	Ag(1)–O(1)	2.503(4)
Ag(1)–N(3a)	2.386(4)	O(3)···O(1)	2.526(6)
Ag(1)–N(2b)	2.394(5)		
N(1)–Ag(1)–N(3a)	109.1(1)	N(1)–Ag(1)–O(1)	128.1(2)
N(1)–Ag(1)–N(2b)	117.7(2)	N(3a)–Ag(1)–O(1)	93.1(1)
N(3a)–Ag(1)–N(2b)	116.0(2)	N(2b)–Ag(1)–O(1)	90.4(2)
Complex **3**			
Ag(1)–N(2a)	2.359(5)	Ag(1)–O(1)	2.519(7)
Ag(1)–N(1)	2.381(6)	O(1)···O(1w)	2.78(1)
Ag(1)–N(4b)	2.402(5)		
N(2a)–Ag(1)–N(1)	111.4(2)	N(1)–Ag(1)–O(1)	92.4(2)
N(2a)–Ag(1)–N(4b)	118.3(2)	N(2a)–Ag(1)–O(1)	126.9(2)
N(1)–Ag(1)–N(4b)	114.8(2)	N(4b)–Ag(1)–O(1)	89.6(2)
Complex **4**			
Ag(1)–N(1)	2.331(6)	Ag(1)–O(1)	2.447(8)
Ag(1)–N(2a)	2.356(6)	O(3)···O(1)	2.468(9)
Ag(1)–N(4b)	2.388(6)	O(1w)···O(2)	2.71(1)
N(1)–Ag(1)–N(2a)	116.1(2)	N(1)–Ag(1)–O(1)	116.6(2)
N(1)–Ag(1)–N(4b)	119.9(2)	N(2a)–Ag(1)–O(1)	82.2(2)
N(2a)–Ag(1)–N(4b)	116.3(2)	N(4b)–Ag(1)–O(1)	97.6(2)

[a] Symmetry codes: (a) $-x + 5/2$, $y - 1/2$, z; (b) x, $y - 1$, z; (c) $-x + 2$, $y - 1/2$, $-z + 1/2$ for **1**; (a) $-x + 3/2$, $y - 1/2$, z; (b) $x - 1/2$, y, $-z + 1/2$; (c) $-x + 1/2$, $y + 1/2$, z for **2**; (a) $-x + 1/2$, y, $z + 1/2$; (b) $-x$, $-y$, $z + 1/2$ for **3**; (a) $-x + 1/2$, $y - 1/2$, z; (b) $-x$, $y - 1/2$, $-z + 1/2$ for **4**.

yield 68%. Anal. calc. for $C_{14}H_{27}Ag_2Cl_2N_9O_8$ **1**: C, 22.84; H, 3.70; N, 17.13%. Found: C, 22.82, H, 3.82; N, 17.15%. IR data (cm^{-1}): 3463m, br, 2926m, 2878m, 2017w, 1649w, 1460m, 1371m, 1239s, 1146vs, 1130vs, 1087vs, 1006vs, 930w, 813s, 688s, 630s, 510m.

[Ag(μ_3-hmt)(ma)] 2. An aqueous solution (5 cm^3) of hmt (0.14 g, 1.0 mmol) was added dropwise to a stirred MeCN–H_2O (2 : 1 *v*/*v*) solution (5 cm^3) of Ag_2(ma) (0.16 g, 0.5 mmol) 50 °C for 15 min. The mixture was dissolved by dropwise addition of aqueous NH_3 solution. The resulting pale yellow solution was allowed to stand in air at room temperature for two weeks, giving colourless crystals in good yield 68%. Anal. calc. for $C_9H_{15}AgN_4O_4$ **2**: C, 30.79; H, 4.31; N, 15.96%. Found: C, 30.72; H, 4.26; N, 16.01%. IR data (cm^{-1}): 3057w, 2966w, 2931w, 1574vs, 1454m, 1405s, 1342m, 1236s, 1046w, 1006vs, 920w, 814m, 738m, 688m, 646m, 625w, 512w.

[Ag(μ_3-hmt)(ba)]·H_2O 3. Compound **3** was prepared as for **1** using Ag(ba) in place of $AgClO_4$ (yield *ca.* 55%). Anal. calc. for $C_{13}H_{19}AgN_4O_3$ **3**: C, 40.33; H, 4.95; N, 14.47%. Found: C, 40.35; H, 5.02; N, 14.32%. IR data (cm^{-1}): 3325m, br, 2938m, 2875m, 1672m, 1595s, 1553vs, 1453w, 1391s, 1229s, 1173w, 1068w, 1004vs, 835w, 814m, 709s, 681s, 512w, 428w.

[Ag(μ_3-hmt)(sal)]·H_2O 4. Compound **4** was prepared as for **1** using Ag(sal) in place of $AgClO_4$ (yield *ca.* 65%). Anal. calc. for $C_{13}H_{19}AgN_4O_4$ **4**: C, 38.73; H, 4.75; N, 13.90%. Found: C, 38.68; H, 4.64; N, 13.75%. IR data (cm^{-1}): 3422m, br, 3067w, 2953m, 2879m, 2691w, 2611w, 1595vs, 1487s, 1462vs, 1390s, 1339m, 1301m, 1235s, 1143m, 1085w, 1053w, 1005vs, 922w, 860m, 811m, 748m, 696m, 668m, 534w, 509w, 463w.

X-Ray crystallography

Diffraction intensities for the four complexes were collected at 21 °C on a Siemens R3m diffractometer using the ω-scan technique. Lorentz-polarization and absorption corrections were applied.[13] The structures were solved by direct methods and refined with the full-matrix least-squares technique using the SHELXS-97 and SHELXL-97 programs, respectively.[14,15] Anisotropic thermal parameters were assigned to all non-hydrogen atoms. The organic hydrogen atoms were generated geometrically (C–H = 0.96 Å); the aqua hydrogen atoms were located from difference maps and refined with isotropic temperature factors. Analytical expressions of neutral-atom scattering factors were employed, and anomalous dispersion corrections were incorporated.[16] The absolute structure for **3** has been determined with a Flack parameter of −0.06(9).[17] Crystal data as well as details of data collection and refinement for the complexes are summarised in Table 1. Selected bond distances and angles are listed in Table 2. Drawings were produced with SHELXTL.[18]

CCDC reference numbers 170950–170953. See http://www.rsc.org/suppdata/nj/b1/b107193a/ for crystallographic data in CIF or other electronic format.

Results

Crystal structures

Complex **1** is made up of two-dimensional infinite highly undulating cationic [Ag(μ_3-hmt)] layers of hexagonal units in a boat-type conformation, which is somewhat similar to the motif found in other [Ag(μ_3-hmt)] layers documented. On the other hand, a mode of interconnection of the hexagonal units in the two-dimensional layers is observed in **1**, resulting in much more undulating two-dimensional layers [Scheme 2(c)]. As illustrated in Fig. 1(a), each hexagonal unit in **1** is organised by three Ag(I) atoms and three hmt ligands at each corner. There are two types of crystallographically independent Ag(I) atoms; Ag(1) is co-ordinated in a trigonal geometry by three nitrogen atoms from different hmt ligands [Ag(1)–N 2.347(5)–2.397(4) Å, N–Ag(1)–N 114.3(2)–124.9(2)°], while Ag(2) is in a distorted tetrahedral geometry co-ordinated by three nitrogen atoms from different hmt ligands [Ag(2)–N 2.349(5)–2.380(5) Å, N–Ag(2)–N 110.6(2)–122.0(2)°] and an MeCN nitrogen atom [Ag(2)–N 2.360(7) Å, N–Ag(2)–N 96.3(3)–102.7(2)°]. The lateral MeCN ligands are oriented above and below the layer [Fig. 1(a)], where they are oriented in an all up/down fashion in each row and an alternately up/down fashion in the columns. It should be noted that the two-dimensional layers in **1** are so undulating that the thickness of the layers is *ca.* 12 Å, as shown in Fig. 1(b). Each pair of MeCN ligands at the same side of the layers are slanted towards each other, resulting in cylindrical channels with a diameter of *ca.* 7.2 Å[19] at both sides of the two-dimensional co-ordination layers. No structure of two-dimensional co-ordination layers containing channels has, to our knowledge, been documented previously. The dimensions of these channels occupy 12.3% of the crystal volume.[20] Unfortunately, half of the perchlorate anions are located in the channels and form acceptor hydrogen bonds [C···O 3.186 and 3.295 Å, C–H···O 120 and 137°] with the hmt methylene groups, thus **1** is not really a microporous material. The remaining perchlorate anions are located between the adjacent layers and form similar hydrogen bonds [C···O 3.228 Å and C–H···O 157°] with the hmt methylene groups, as shown as Fig. 1(c).

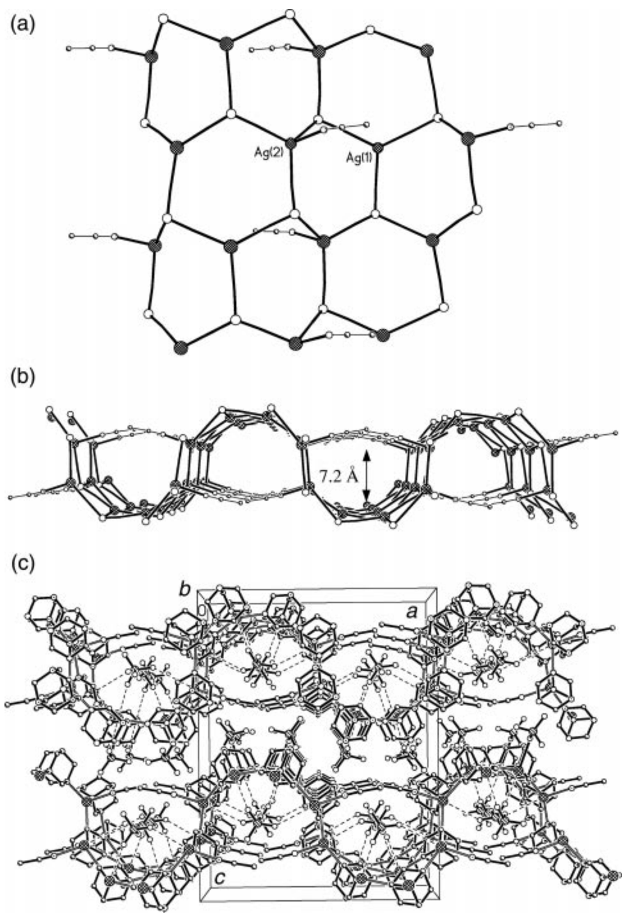

Fig. 1 Perspective views of a layer viewed from the top (a) and side (b), and packing of the layers viewed along the *b*-axis (c) in **1**. For clarity, the hmt ligands in (a) and (b) are simplified as open circles at their centres of mass.

Complex **2** is also made up of two-dimensional infinite, highly undulating layers of hexagonal units in a boat-type conformation, where the interconnection fashion of the hexagonal units, as illustrated Scheme 2(d), is slightly different from those found in **1** and the related compounds reported previously. In contrast to **1** there is only one kind of crystallographically independent Ag(I) atom, which is co-ordinated in a distorted tetrahedral geometry by three nitrogen atoms [Ag(1)–N 2.345(4)–2.394(5) Å, N–Ag(1)–N 109.1(1)–117.7(2)°] from different hmt ligands and one monodentate ma ligand [Ag(1)–O 2.503(4) Å, O–Ag(1)–N 90.4(2)–128.1(2)°]. As shown in Fig. 2(a), the ma ligands are oriented in an alternately up/down fashion in both the rows and columns, unlike those in **1**. Similarly to **1**, each pair of lateral ma ligands at the same side of the layers are also slanted towards each other, resulting in cylindrical channels at both sides of the two-dimensional co-ordination layers [Fig. 2(b)]. Each pair of ma ligands are further interlinked by a strong hydrogen bonds [O(1)···O(3) 2.526(6) Å] between the protonated carboxylic oxygen atoms and a co-ordinated carboxylate oxygen atom [Fig. 2(a)]. Due to the branching ma ligands, a micropore-shaped rather than an effective micropourous structure is now generated, in which the 'channel' size in **2** is much smaller than that in **1**, and no guest molecules are clathrated within.

Similarly to **2**, both **3** and **4** also consist of two-dimensional infinite highly undulating neutral layers of hexagonal units, in which each unit is also organised by three Ag(I) atoms and three hmt ligands at each corner (Fig. 3). The Ag(I) atom is in a distorted tetrahedral geometry co-ordinated by three nitrogen atoms from different hmt ligands [Ag(1)–N 2.359(5)–2.402(5) Å, N–Ag(1)–N 111.4(2)–118.3(2)° in **3**; Ag(1)–N 2.331(6)–2.388(6) Å, N–Ag(1)–N 116.1(2)–119.9(2)° in **4**] and one oxygen atom from one monodentate aromatic carboxylate [Ag(1)–O 2.519(7) Å, N–Ag(1)–O 89.6(2)–126.9(2)° in **3**; Ag(1)–O 2.447(8) Å, N–Ag(1)–O 82.2(2)–116.6(2)° in **4**]. The interconnection of the hexagonal units and the orientation of the lateral aromatic carboxylates of the layers in both **3** and **4** are similar to those in **2**. Each pair of aromatic carboxylates at the same side of the layers are slanted towards each other, resulting in cylindrical channels with an effective diameter of *ca.* 4.0 Å at both sides of the two-dimensional layers. Significant C–H···π interactions between the aromatic carboxylate pairs are observed, since the edge-to-face separations of the adjacent aromatic rings are 3.74 and 3.68 Å for **3** and **4**, respectively. Although the free dimensions of these channels occupy only 5.4% of the total volume in **3** and **4**, they are true porous materials, as evidenced by their inclusion of guest water molecules. Each guest water molecule forms a donor hydrogen bond with the co-ordinated carboxylate oxygen atom [O(1w)···O(1) 2.78(1) Å in **3** and O(1w)···O(2) 2.71(1) Å in **4**], and further forms an acceptor C–H···O hydrogen bond with the hmt methylene group [C(4)···O(1w) 3.323 Å, and C(4)–H···O(1w) 120° in **3**; C(3)···O(1w) 3.295 Å, and C(3)–H···O(1w) 153° in **4**]. It should be noted that the two-dimensional layers are stacked through van der Waals interactions into the three-dimensional molecular architectures in **3** and through moderately strong, offset π–π stacking interactions between the aromatic rings from adjacent layers with a face-to-face distance of *ca.* 3.76 Å in **4**.

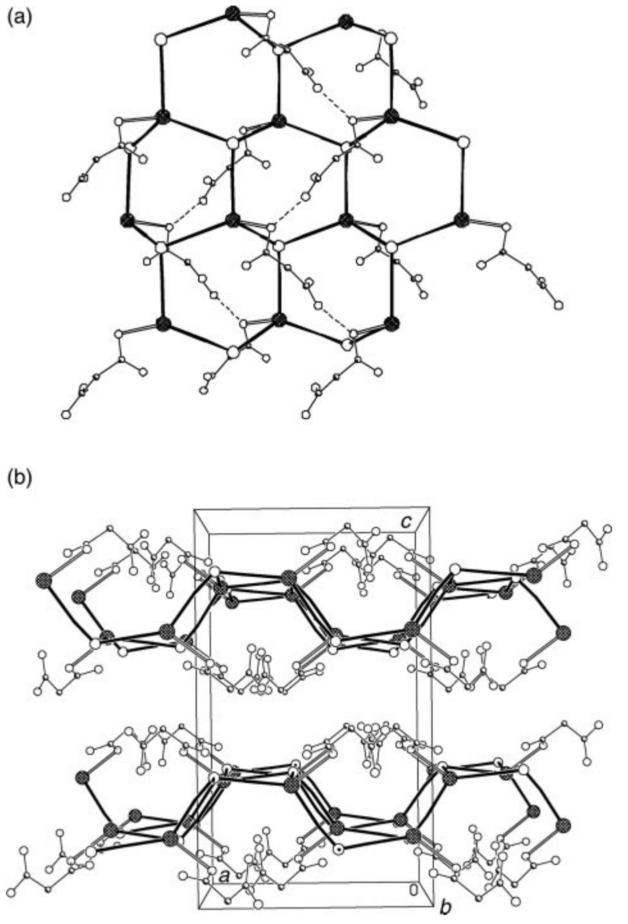

Fig. 2 Perspective view of a layer viewed from the top (a) and packing of the layers viewed along the *b*-axis (b) in **2**. For clarity, the hmt ligands are simplified as open circles at their centres of mass.

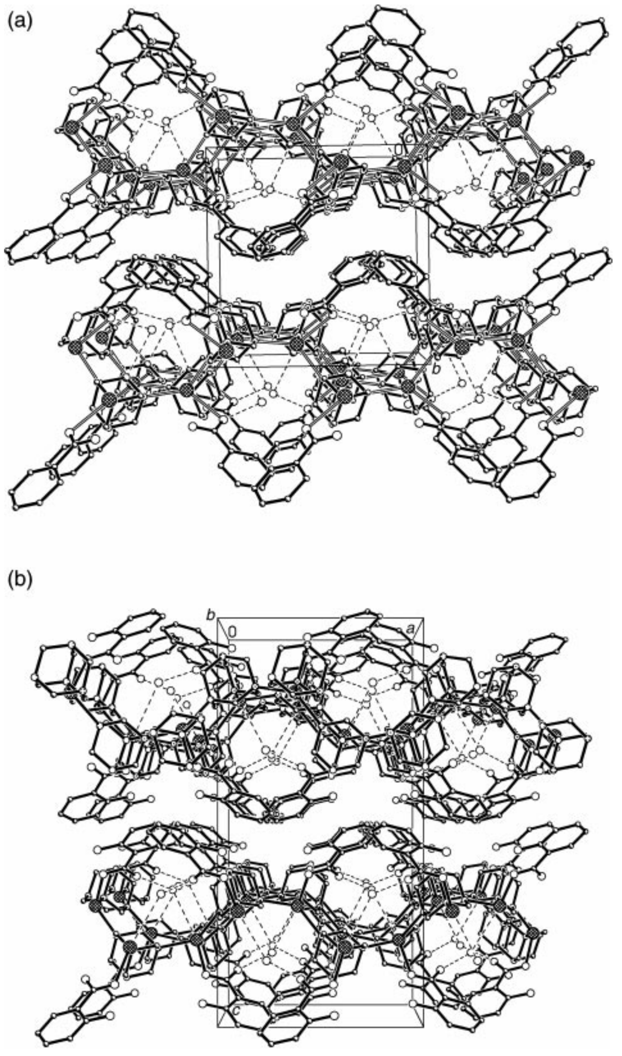

Fig. 3 Perspective views of the packing of the layers viewed along the *a*-axis in **3** (a) and along the *b*-axis in **4** (b).

Thermogravimetric analyses

In order to examine the thermal stability of these porous networks, thermogravimetric analyses (TGA) were carried out. The samples were heated up to 600 °C in N_2. The TGA curve for **1** shows that the first weight loss of 5.8% between 120 and 160 °C corresponds to the loss of one acetonitrile molecule (calculated: 5.6%). Decomposition of the polymeric framework of **1** began at >200 °C, while that of **2** began at >210 °C. The TGA curves for **3** and **4** are very similar, showing first weight losses of 4.4 and 4.8% between 70 and 140 °C corresponding to the loss of one lattice water molecule per mol for **3** (calculated: 4.6%) and **4** (calculated: 4.5%), respectively. Both **3** and **4** were decomposed at >210 °C. The polymeric networks of **1**–**4** are quite stable, they may be, in a sense, related to porous materials.

Discussion

We and others have previously reported many kinds of Ag–hmt supramolecular architectures, and more than half consist of two-dimensional [Ag(μ_3-hmt)] layers of hexagonal units in a boat-type conformation. However, different modes of interconnection between the hexagonal units in the [Ag(μ_3-hmt)] layers have not been discussed so far. A careful examination of detailed geometric data for the complexes comprised of two-dimensional [Ag(μ_3-hmt)] layers with hexagonal units reveals that there are four types of molecular topologies (see Scheme 2), two of which are found in this work [Scheme 2(c, d)]. We have also found that in the [Ag(μ_3-hmt)X] layer complexes with slanted lateral X ligands reported previously [X = 1-hydroxy-2-naphthate, 3-hydroxy-2-naphthate and 2-naphthoxyacetate, see Scheme 2(b)][10] and those in this work [Scheme 2(d)], the Ag–O bonds are much longer than the Ag–N ones. In contrast, the Ag–O bonds are shorter than the Ag–N ones in the [Ag(μ_3-hmt)X] complexes with perpendicular lateral X ligands [X = 3-nitrobenzoate, 4-nitrobenzoate and 3,5-dinitrobenzoate, see Scheme 2(a)].[10] This fact shows that the bonding interactions between the Ag(I) atoms and the lateral ligands in **2**–**4** are somewhat weak, which may be responsible for the different interconnection modes of the hexagonal units, the slanted orientation of the lateral ligands as well as the different slanted orientations, as shown in Scheme 2(b, d). Moreover, the large naphthate groups in the previously reported complexes may exclude their orientation in a similar fashion to that found in **2**–**4** due to the mutual repulsion between the naphthate groups. On the other hand, the similar layer topology in **1** may be ascribed to the fact that, though the lateral MeCN ligand is a stronger ligand, there are trigonally co-ordinated Ag(I) centres in the layer. Such three-co-ordinate centres alter the interconnection made of the hexagonal units.

In summary, we have synthesised four new Ag–hmt complexes in which the two-dimensional [Ag(μ_3-hmt)] layers of hexagonal units in a boat-type conformation are highly undulating and each pair of adjacent lateral ligands, either MeCN or carboxylates, at the same side of the layers are slanted towards each other, resulting in new two-dimensional co-ordination frameworks containing micropores. This work suggests a new strategy for the construction of microporous metal–organic materials.

Acknowledgements

This work was supported by the National Natural Science Foundation of China (grant no. 29971033 and 20001008) and the Foundation for University Key Teachers of the Ministry of Education of China. We are also indebted to the Chemistry Department of The Chinese University of Hong Kong for donating the diffractometer.

References and notes

1 C. Janiak, *Angew. Chem., Int. Ed. Engl.*, 1997, **36**, 1431; S. R. Batten and R. Robson, *Angew. Chem., Int. Ed.*, 1998, **37**, 1460; O. M. Yaghi, H. Li, C. Davis, D. Richardson and T. L. Groy, *Acc. Chem. Res.*, 1998, **31**, 474; M. Munakata, L. Wu and T. Kuroda-Sowa, *Adv. Inorg. Chem.*, 1999, **46**, 173; S. Kitagawa and M. Kondo, *Bull. Chem. Soc. Jpn.*, 1998, **71**, 1735; A. J. Blake, N. R. Champness, P. Hubberstey, W.-S. Li, M. A. Withersby and M. Schröder, *Coord. Chem. Rev.*, 1999, **183**, 117; P. J. Hagrman, D. Hagrman and J. Zubieta, *Angew. Chem., Int. Ed.*, 1999, **38**, 2639.

2 C. A. Hunter, *Angew. Chem., Int. Ed. Engl.*, 1995, **34**, 1079.

3 M. Eddaoudi, H. Li and O. M. Yaghi, *J. Am. Chem. Soc.*, 2000, **122**, 1391; M. Kondo, T. Yoshitomi, K. Seki, H. Matsuzaka and S. Kitagawa, *Angew. Chem., Int. Ed. Engl.*, 1997, **37**, 1725; T. M. Reineke, M. Eddaoudi, M. O'Keeffe and O. M. Yaghi, *Angew. Chem., Int. Ed.*, 1999, **38**, 2590; H. Li, M. Eddaoudi, M. O'Keeffe and O. M. Yaghi, *Nature*, 1999, **402**, 276; S.-I. Noro, S. Kitagawa, M. Kondo and K. Seki, *Angew. Chem., Int. Ed.*, 2000, **39**, 2081; H. Li, M. Eddaoudi, T. L. Groy and O. M. Yaghi, *J. Am. Chem. Soc.*, 1998, **120**, 8571.

4 M.-L. Tong, X.-L. Yu, X.-M. Chen and T. C. W. Mak, *J. Chem. Soc., Dalton Trans.*, 1998, 5; M.-L. Tong, B.-H. Ye, J.-W. Cai, X.-M. Chen and S. W. Ng, *Inorg. Chem.*, 1998, **37**, 2645; M.-L. Tong, H. K. Lee, X.-M. Chen, R.-B. Huang and T. C. W. Mak, *J. Chem. Soc., Dalton Trans.*, 1999, 3657; M.-L. Tong, X.-M. Chen, B.-H. Ye and L.-N. Ji, *Angew. Chem., Int. Ed.*, 1999, **38**, 2237; M.-L. Tong, H.-J. Chen and X.-M. Chen, *Inorg. Chem.*, 2000, **39**, 2235; S.-P. Yang, X.-M. Chen and L.-N. Ji, *J. Chem. Soc., Dalton Trans.*, 2000, 2337; H.-J. Chen, L.-Z. Zhang, Z.-G. Cai, G. Yang and X.-M. Chen, *J. Chem. Soc., Dalton Trans.*, 2000, 2463; M.-L. Tong, X.-M. Chen and S. W. Ng, *Inorg. Chem. Commun.*, 2000, **3**, 436.

5 L. Carlucci, G. Ciani, D. M. Proserpio and A. Sironi, *J. Am. Chem. Soc.*, 1995, **117**, 12861; L. Carlucci, G. Ciani, D. M. Proserpio and A. Sironi, *Inorg. Chem.*, 1997, **36**, 1736; L. Carlucci, G. Ciani, D. W. V. Gudenberg, D. M. Proserpio and A. Sironi, *Chem. Commun.*, 1997, 631; M. Bertelli, L. Carlucci, G. Ciani, D. M. Proserpio and A. Sironi, *J. Mater. Chem.*, 1997, **7**, 1271.

6 L. Carlucci, G. Ciani, D. M. Proserpio and S. Rizzato, *J. Solid State Chem.*, 2000, **152**, 211.

7 A. Michelet, B. Voissat, P. Khodadad and N. Rodier, *Acta Crystallogr., Sect. B*, 1981, **37**, 2171.

8 O. M. Yaghi, H. Li and M. O'Keeffe, *Mater. Res. Symp. Proc.*, 1997, **453**, 127.

9 M.-L. Tong, S.-L. Zheng and X.-M. Chen, *Chem. Commun.*, 1999, 561; M.-L. Tong, S.-L. Zheng and X.-M. Chen, *Chem. Eur. J.*, 2000, **6**, 3729.

10 S.-L. Zheng, M.-L. Tong, R.-W. Fu, X.-M. Chen and S. W. Ng, *Inorg. Chem.*, 2001, **40**, 3562.

11 S.-L. Zheng, M.-L. Tong, X.-L. Yu and X.-M. Chen, *J. Chem. Soc., Dalton Trans.*, 2001, 586; S.-L. Zheng, M.-L. Tong, H.-L. Zhu, Y. Fang and X.-M. Chen, *J. Chem. Soc., Dalton Trans.*, 2001, 2049.

12 T. C. W. Mak, W.-H. Yip, C. H. L. Kennard, G. Smith and E. J. O'Reilly, *Aust. J. Chem.*, 1986, **39**, 541.

13 A. C. T. North, D. C. Phillips and F. S. Mathews, *Acta Crystallogr., Sec. A*, 1968, **24**, 351.

14 G. M. Sheldrick, SHELXS-97, Program for Crystal Structure Solution, Göttingen University, Germany, 1997.

15 G. M. Sheldrick, SHELXL-97, Program for Crystal Structure Refinement, Göttingen University, Germany, 1997.

16 D. T. Cromer, International Table for X-ray Crystallography, Kluwer Academic Publishers, Dordrecht, 1992, vol. C, Tables 4.2.6.8 and 6.1.1.4.

17 H. D. Flack, *Acta Crystallogr., Sect. A*, 1983, **39**, 876.

18 G. M. Sheldrick, SHELXTL, Version 5, Siemens Industrial Automation Inc., Madison, WI, USA, 1995.

19 Hereafter, the channel dimensions are estimated from the van der Waals radii for carbon (1.70 Å), nitrogen (1.55 Å) and oxygen (1.40 Å).

20 A. L. Spek, PLATON, A Multipurpose Crystallographic Tool, Untrecht University, The Netherlands, 1999.